Composites: Part B 45 (2013) 50–62

Contents lists available at SciVerse ScienceDirect

Composites: Part B

journal homepage: www.elsevier.com/locate/compositesb

Model-based damage reconstruction in composites from ultrasound transmission

Ahmed A. Fahim, Rafael Gallego, Nicolas Bochud, Guillermo Rus *

Department of Structural Mechanics, University of Granada, Politécnico de Fuentenueva, 18071 Granada, Spain

ARTICLE INFO

Article history:
Received 22 September 2011
Received in revised form 7 August 2012
Accepted 1 September 2012
Available online 17 September 2012

Keywords:
A. Carbon–carbon composites (CCCs)
B. Mechanical properties
C. Analytical modelling
D. Ultrasonics
Inverse problem

ABSTRACT

Composites are high performance advanced materials with a growing applicability due to their extreme strength, rigidity to weight ratios. However, usual kinds of damage are hardly visible and require monitoring techniques to guarantee their reliability. Impact-type damage, which may occur during manufacture, service or maintenance, can induce severe degradation of the mechanical properties to composite materials by delamination, matrix cracking and fiber breakage while remaining invisible from the surface.

This work aims to design and develop experimentally a non-destructive monitoring technique based on ultrasonic transmission through thickness combined with a model-based inverse problem for detecting variations in structural parameters due to impact damage. A model-based inverse problem is proposed using a semi-analytical model of the ultrasonic wave propagation in the layered composite material. Once calibrated, this model simulates the response of the excitation – propagation – measurement system and the wave-damage interaction for the assumed types of continuum damage. The damage parameters and the mechanical constants of the laminated composite material are obtained by minimizing a cost functional that quantifies the mismatch between experimental and simulated measurements. These parameters can be correlated with the damage condition. Genetic algorithms are used as parameter search algorithms due to their capability of finding a global solution where the cost functional has several local minima that may give false answers, at the cost of larger computational resources than gradient-based algorithms.

Finally, a sensitivity study to the uncertainties of the parameters is performed for establishing the feasibility of this technique. The reconstruction procedure using genetic algorithms is proved feasible to quantify mechanical damage properties from a single measurement.

1. Introduction

One of the major concerns associated with composites is the vulnerability to impact damage, which may occur during manufacture, service or maintenance. Impacts can induce serious damage to composites such as delamination, matrix cracking and fiber breakage. Although such damage is hardly visible, it can severely degrade the mechanical properties and the load carrying capability of the structure [24]. The severity of impact damage can be significantly reduced by the use of tougher fiber matrix materials. However, for safe life and damage-tolerant composite structures, the problem of impact damage detection is of ongoing importance [31].

Over the last decades, several models have been proposed to describe the multiple damage mechanisms of composites. The mechanical behavior of matrix cracked laminates was modeled by Talreja [32,33] and Allen et al. [1] in terms of continuum damage theory. This stiffness reduction model involves a set of unknown ply damage constants, which must be determined experimentally. Allen and Lee [2] derived approximated relations between the internal damage state variables and laminate stiffness for cross-ply laminates. The variational approach for matrix cracking was developed by Hashin [11]. This approach has been implemented and extended by several other researchers including [21].

At low energy impact, the damage is not always visible on the impacted surface but starts on the opposite surface and then propagates internally. This makes defect detection from the impacted surface, often the only accessible side for investigation, a challenging task. For an early and accurate detection of these defects, especially the ones related to low-velocity impact, extremely sensitive probes are required. Single-side inspection probes are obviously preferred. Impact damage is considered as the primary cause of in-service delamination in composites. Delaminations can reduce the compressive strength of the material, while fiber fracture and matrix cracking reduce the static residual strength. Thus, the capability to discriminate between the different failure mechanisms during inspection is a requirement for the non-destructive

* Corresponding author. Tel./fax: +34 958249482.
E-mail address: grus@ugr.es (G. Rus).

1359-8368/$ - see front matter © 2012 Elsevier Ltd. All rights reserved.
http://dx.doi.org/10.1016/j.compositesb.2012.09.003

evaluation (NDE) technique used on these materials [26]. Olsson et al. [22] provides a simplified formula to establish the threshold impact loading to generate a delamination, which is validated by FEM and experimentally against other authors. Also a continuum damage model combining delamination and fiber breakage is proposed and experimented by Williams et al. [38].

Ultrasound for inspecting damage is particularly useful since ultrasound pulses are mechanical waves, whose propagation is governed by the elasticity equations and therefore most sensitive to their mechanical constants, which are responsible for the final structural health. Mal et al. [18] presents a good review of many of the early NDE techniques for monitoring the integrity of fiber-reinforced plastic composites. Recently, Shen et al. [30] carefully reviews the ultrasonic NDE techniques for impact damage inspection of CFRP laminate. Chang et al. [5] modeled the propagation of 100 MHz ultrasonic waves through a matrix with fibers using finite elements, visualizing the complex interactions and dissipation between them, which clarifies the reason why detailed damage investigation is complicated using ultrasonics. The relationship between damage and attenuation parameters was experimentally studied by Kyriaglozou and Guild [13] in vibration testing of CFRP with notches, using Rayleigh damping coefficients as damage parameters in a FEM model. In our previous studies [3,7], signal processing techniques were successfully applied to discriminate between several impact damages on a CFRP plate, by extracting features from the ultrasonic measurements.

To understand the nature of the damage at the microstructural level, the appearance of microvoids can be interpreted in light of the theory proposed by Yeh and Cheng [41] that correlates the Mori and Tanaka [19] damage predicted by FEM with the damage derived from the elastic constants reduction measured by ultrasound.

The use of numerical models of the propagation of ultrasound through composites and their interaction with damage and delaminations for their characterization has scarcely been addressed. A theoretical framework to define a consistent approach is the model-based inverse problem solution [35]. Direct search methods, such as neural networks, genetic algorithms and simulated annealing methods are developed and promisingly applied to the field of structural identification. Among them, genetic algorithms (GA) [10] attract our attention because of the fact that the technique requires significantly small amount of data in dealing with complex problems, while attaining global convergence as opposed to gradient-based methods. Yang et al. [40] presented an inverse procedure for the detection of a three-dimensional crack in plates and shells using a genetic search algorithm using the integral strain measured by optical fibers. Nag et al. [20] proposed an efficient strategy for identification of delamination in composite beams and connected structures using a GA integrated with finite-element code for automation. Xu and Liu [39] proposed a method of damage detection for composite plates using Lamb waves and a projection GA. The projection genetic algorithm was developed from the hybridization of a modified micro-genetic algorithm with a projection operator. Recently, techniques for detecting damages from noisy static or dynamic responses of anisotropic plates are evolving. Lee and Wooh [16,17] applied an advanced micro-genetic algorithm for detecting damage of steel and composite structures subjected to impact load. Rus et al. [27] dealt with a method of damage detection for plane stress problem of composites using boundary element method (BEM). However, all these works are limited in that they can analyze only homogenized damage, and not its distribution along layers and delaminations. Moreover, most of the works dedicated to the resolution of IP's are purely theoretics, whereas the experimental measurements are simulated by making use of the numerical model (by inserting some random or convolutional noise).

This work aims to develop a non-destructive monitoring system based on the use of ultrasonic through-transmission of primary waves in composite materials, for detecting and quantifying the variations of structural parameters due to impact damage. Local NDE techniques in thin layers traditionally avoid conventional methods such as the pulse-echo, pulse transfer or resonance [42], since high-frequency waves highlight high attenuation phenomena. In order to prevent those inconveniences, a low-frequency transmission setup is proposed, where primary waves are traveling through a specimen whose layers are smaller than the corresponding wavelength, as described by Kinra and Iyer [12]. The simulation of the system is proposed using a semi-analytical model of the propagation and interactions of the ultrasonic waves within the multilayered composites. The mechanical and geometrical properties (thickness, elastic modulus, Poisson-ratio, density and attenuation coefficient) of the different layers are then identified by minimizing the discrepancy between experimental measurements and numerically predicted results, by updating successively the model during the iterative search algorithm [28,14,15]. Genetic algorithms are used as search algorithms during the optimization procedure, providing enhancements on the inversion and physical interpretation of the resulting damage parameters. The latter are then correlated with the damage conditions.

The presented monitoring technique achieves for the first time the reconstruction of multiple damages from a single measurement. The methodology is physics-based through a computational model of ultrasound-damage interaction. In contrast to other studies, the damage is not identified by considering the time-of-flight or the broadband ultrasound attenuation, but by reconstructing the complete waveform. Moreover, the damage multiplicity does not only appear at several locations (layers) but simultaneously in different forms (layer degradation and interlaminar debonding). The feasibility of the model is validated both experimentally and numerically by a sensitivity analysis.

2. Methodology

2.1. Composites mechanical properties characterization

Several mechanical and geometrical properties of the laminate specimens were unknown after manufacture. They were therefore characterized by burning off the resin in an oven at 500 °C during approximately 16 h. The images of each burned piece were introduced in AutoCAD software by marking the axis of reference and measuring the angle of each layer, in order to count the number of layers in each specimen, weighting the carbon fibers of each layer, measuring the thickness of each layer by digital media, and the angles of the fibers with regard to the longitudinal axis of the specimen. This data set allowed us to calculate the density and elastic constants of the resin, the carbon and the fraction of volume of fiber of each layer and each specimen, as a function of the

Table 1
Main mechanical properties of specimen A and C.

	Specimen A	Specimen C	Unit
Total weight	275.1000	265.1000	(mg)
Total volume	191.2928	128.7195	(mm^3)
Total density	1.4381	2.0595	(g/ml)
Carbon weight	195.4000	135.2000	(mg)
Carbon density	2.2600	2.2600	(g/ml)
Carbon volume	86.4602	59.8230	(mm^3)
Matrix weight	79.7000	129.9000	(mg)
Matrix volume	104.8326	68.8965	(mm^3)
Matrix density	0.7603	1.8854	(g/ml)

polymer matrix elastic constants, which were later calibrated by ultrasound measurements, summarized in Table 1.

As the specimen A and C present symmetrical structure, the average density and the average percentage of fibers of the symmetric layers was calculated, as summarized in Tables 2 and 3.

2.2. Generation of damage in specimens

Damage were generated by applying various free-fall impact energies according to the mass and height of each impactor, as illustrated in Fig. 1.

Table 4 summarizes the characteristics of each impactor used to damage the composite plates.

Table 2
Summary of specimen A characteristics used in the numerical model.

Average density between layer 1 and 5	1.8747	(g/ml)
Average %fiber between layer 1 and 5	0.7431	
Average young modulus between layer 1 and 5	10.2115	(GPa)
Average Poisson ratio between layer 1 and 5	0.2937	
Average density between layer 2 and 4	1.4564	(g/ml)
Average %fiber between layer 2 and 4	0.4642	
Average young modulus between layer 2 and 4	6.7419	(GPa)
Average Poisson ratio between layer 2 and 4	0.3148	
Young modulus without fibers	3.4	(GPa)

Table 3
Summary of specimen C characteristics used in the numerical model.

Average density between layer 1 and 4	2.0543	(g/ml)
Average %fiber between layer 1 and 4	0.4508	
Average young modulus between layer 1 and 5	6.5675	(GPa)
Average Poisson ratio between layer 1 and 5	0.3158	
Average density between layer 2 and 3	2.0654	(g/ml)
Average %fiber between layer 2 and 3	0.4806	
Average young modulus between layer 2 and 3	6.8586	(GPa)
Average Poisson ratio between layer 2 and 3	0.3136	
Young modulus without fibers	3.4	(GPa)

2.3. Ultrasonic testing setup and measurements

Ultrasonics are high frequency mechanical waves, and are therefore suited for characterizing elastic moduli. Parameters such as Rayleigh damping, density and elastic modulus, have all been demonstrated feasible for the inspection of the condition of a material or a structure. The velocity and attenuation variation is dependent on the frequency and elastic constants of the layers that the wave travels through. These parameters are combined for the different layers and generate a waveform that needs to be processed by a complete inversion scheme. For best measuring the velocity and attenuation, a transmission setup with a low-frequency ultrasonic pulse containing a wide range of frequencies and a high power of penetration is adopted.

The testing system used in the experimental phase of this study is composed of six main units. They are (1) an electric pulse generator, (2) two transducers, (3) coupling medium gel, (4) an oscilloscope, (5) an amplifier and pre-amplifier, and (6) a personal computer as illustrated in Fig. 2.

The specimen was excited by low-frequency ultrasonic burst waves at a central frequency of 5 MHz, amplitude of 10 mV, one cycle at period of 100 μs. The response was measured at a point without damage for the calibration, and the digitalization configuration is characterized by a vertical scale of 400 mV and a time scale of 500 ns, as highlighted in Fig. 3.

For each damage level, the measurements have been repeated several times to account for the uncertainties due to the variability of the distance from the center of the damage, the pressure with which the transducers have been subjected, and the goodness of the alignment between them, as illustrated in Fig. 4.

2.4. Numerical model

A numerical simulation of the experimental system is proposed using a semi-analytical model of the wave interaction with layers and damage based on the *transfer matrix formalism*, describing the ultrasonic waves propagation in multilayered composites.

Fig. 1. Impactors and specimens used in the experiments.

Table 4
Impactors for the generation of damage.

Impactor	Weight (g)	Height (m)	Energy (J)
1	17.11	2.315	0.388
1	17.11	4.018	0.674
2	57.85	4.018	1.313
2	57.85	2.315	2.280
3	136.62	2.315	3.102
3	136.62	4.018	5.385
4	463.11	2.315	10.517
4	463.11	4.018	18.54

The following assumptions are proposed for the numerical approach: (i) perfect bonding between fibers and matrix exists, (ii) fibers are parallel and uniformly distributed throughout, (iii) the matrix is free of voids or microcracks and initially in a stress-free state, (iv) both fibers and matrix are isotropic and obey Hooke's law, and (v) the applied loads are perpendicular to the fiber [25]. The general scheme of the numerical procedure is based on the block's diagram depicted in Fig. 5.

A major damage mode in composites is delamination. This mode has been approximated by the model as an interface layer of much smaller thickness than both plies and wavelength, whose transversal elastic modulus is linearly decreased by a damage parameter. Let us first consider the longitudinal plane wave equation along the x_3-axis of a thin elastic medium,

$$\ddot{u}(x_3,t) = c_p^2 u''(x_3,t) \tag{1}$$

where c_p denotes the primary wave velocity. $\ddot{u}(x_3,t)$ and $u''(x_3,t)$ are the second time-derivatives and second derivatives with respect to the x_3-coordinate, respectively. The displacement $u(x_3,t)$ can be expressed in terms of its Fourier transform $\tilde{u}(x_3,\omega)$ (by dropping the time factor $e^{i\omega t}$, with angular frequency ω) as,

$$u(x_3,t) = \frac{1}{\sqrt{2\pi}} \int_{-\infty}^{\infty} \tilde{u}(x_3,\omega) e^{-i\omega t}\, d\omega \tag{2}$$

and thus, a general solution can be stated in the frequency-domain as,

$$\tilde{u}(x_3,\omega) = \tilde{u}^f(x_3,\omega) + \tilde{u}^b(x_3,\omega) = Ae^{-ikx_3} + Be^{ikx_3} \tag{3}$$

where $\tilde{u}^f(x_3,\omega)$ and $\tilde{u}^b(x_3,\omega)$ stand for the forward- and backward-propa-gating parts of the linear displacement $\tilde{u}(x_3,\omega)$, respectively. k denotes the complex wave number, which accounts for attenuation. In a further step, this solution is decomposed in each harmonic component $\tilde{u}^{(n)}(x_3,\omega)$, with respect to the natural frequency. The upper index (n) denotes the order of the considered harmonic component, defined as $n = F_s/N_s$, where F_s and N_s denote the sampling frequency and number of samples, respectively. Let us consider sharp discontinuities between N homogeneous linear-elastic media with the same cross-sections. Hence,

$$\tilde{u}_m^{(n)}(x_3,\omega) = A_m^{(n)} e^{-ink_m x_3} + B_m^{(n)} e^{ink_m x_3} \tag{4}$$

where the subindex m denotes the material in which the waves are propagating. The calculation of the transfer matrix is based on specific transmission conditions, which depend on the perfect or imperfect interface between the layers. In the case of perfectly bonded interface, the transmission conditions imply the continuity of displacement $\tilde{u}_m^{(n)}(x_3,\omega)$ and stress $\tilde{\sigma}_m^{(n)}(x_3,\omega)$ across the interface [6]. Making use of these conditions at an arbitrary interface $x_3 = d_m$,

$$\begin{aligned} \tilde{u}_m^{(n)}(d_m,\omega) &= \tilde{u}_{m+1}^{(n)}(d_m,\omega) \\ \tilde{\sigma}_m^{(n)}(d_m,\omega) &= \tilde{\sigma}_{m+1}^{(n)}(d_m,\omega) \end{aligned} \tag{5}$$

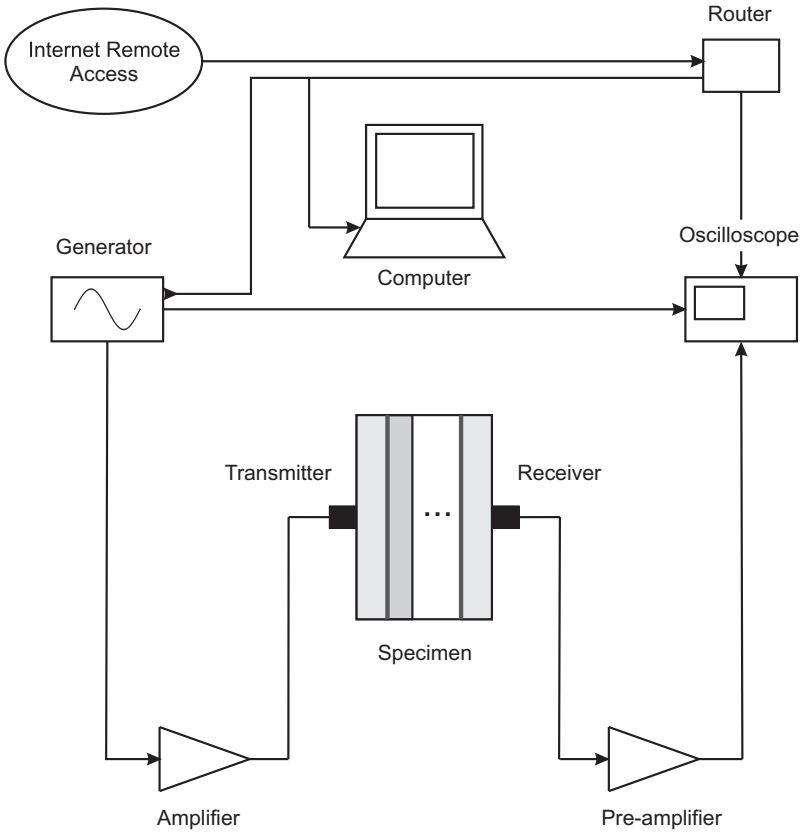

Fig. 2. The experimental setup and the connections of the main units.

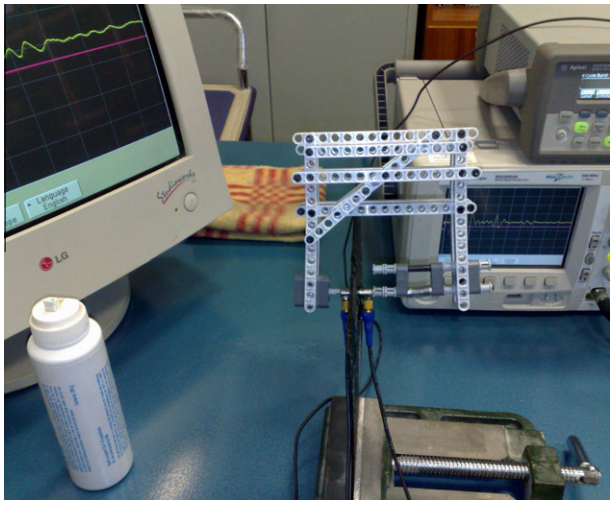

Fig. 3. The experimental measurements realized in the laboratory.

a hard transition from a layer m to a layer $m+1$ can be characterized by the *discontinuity matrix* $D_{m,m+1}$,

$$\widetilde{U}^{(n)}_{m+1}(d_m,\omega) = D^{(n)}_{m,m+1}\widetilde{U}^{(n)}_{m}(d_m,\omega) \tag{6}$$

where the state vector is denoted by $\widetilde{U}^{(n)}_i = [\tilde{u}^{(n),f}_i \ \tilde{u}^{(n),b}_i]^T$. The *discontinuity matrix* depends only on the acoustic impedances $Z_i = \rho_i c_i$ of the two layers being in contact, leading to

$$D^{(n)}_{m,m+1} = \frac{1}{2}\begin{pmatrix} 1+\frac{Z_m}{Z_{m+1}} & 1-\frac{Z_m}{Z_{m+1}} \\ 1-\frac{Z_m}{Z_{m+1}} & 1+\frac{Z_m}{Z_{m+1}} \end{pmatrix} \tag{7}$$

Considering a harmonic pulse propagating in the same homogeneous layer m from position $x_3 = d_{m-1}$ to position $x_3 = d_m$, its transformed displacement at the respective locations can be expressed by the *propagation matrix* P_m,

$$\widetilde{U}^{(n)}_{m}(d_m,\omega) = P^{(n)}_{m}\widetilde{U}^{(n)}_{m}(d_{m-1},\omega) \tag{8}$$

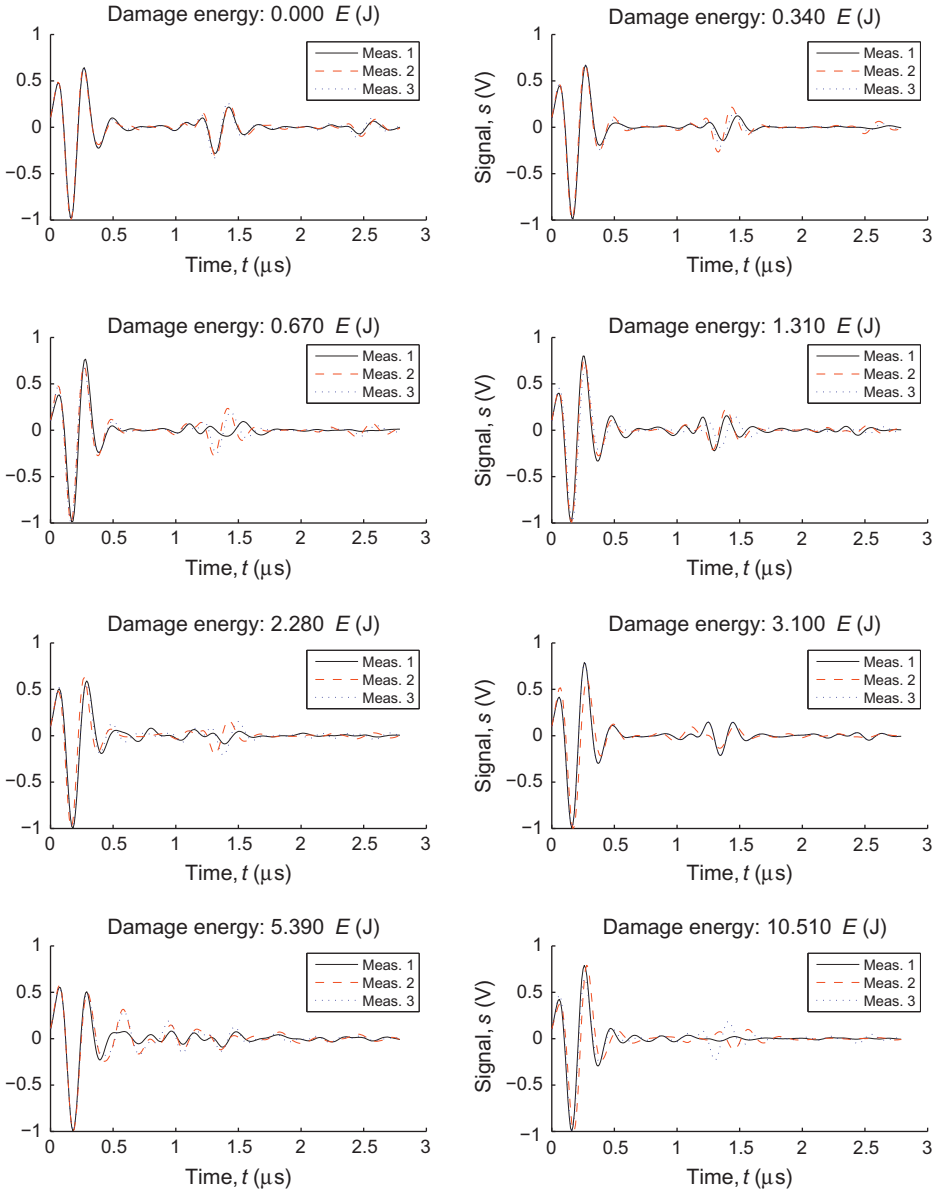

Fig. 4. Comparison between experimental measurements/damage level.

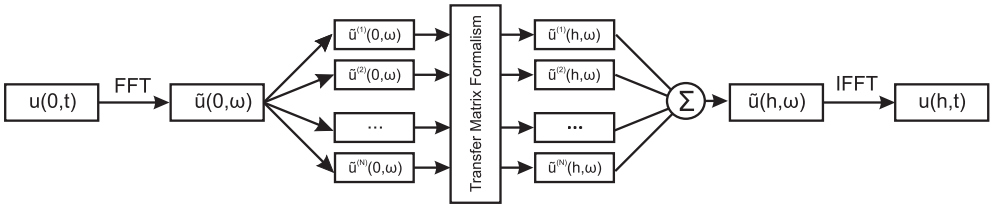

Fig. 5. General scheme of the numerical procedure.

with

$$P_m^{(n)} = \begin{pmatrix} e^{-ink_m a_m} & 0 \\ 0 & e^{ink_m a_m} \end{pmatrix} \tag{9}$$

where $a_m = d_m - d_{m-1}$ is the thickness of the layer/interface m. Through combination of *discontinuity* and *propagation matrices*, it is possible to describe a succession of transitions, and expressions for the reflection and transmission processes at a multilayered transition can be obtained. The advantage of this formalism can be highlighted considering wave propagation through periodic or symmetric material transition. Considering so far only the case of interest, namely a one-dimensional longitudinal plane wave propagating from excitation point $x_3 = 0$ to detection point $x_3 = h$ within a thin linear elastic medium composed of N homogeneous layers, the *transfer matrix* $T^{(n)}$ gives a relation between the input and the output state vectors as

$$\begin{pmatrix} \tilde{u}_N^{(n),f}(h,\omega) \\ \tilde{u}_N^{(n),b}(h,\omega) \end{pmatrix} = T^{(n)}(k_m, a_m, Z_m) \cdot \begin{pmatrix} \tilde{u}_1^{(n),f}(0,\omega) \\ \tilde{u}_1^{(n),b}(0,\omega) \end{pmatrix} \tag{10}$$

where the *transfer matrix* can be obtained as the successive products of *propagation* and *discontinuity matrices*:

$$T^{(n)}(k_N, a_N, Z_N) = \left[\prod_{j=0}^{N-2} P_{N-j}^{(n)} D_{N-j-1,N-j}^{(n)} \right] P_1^{(n)} \tag{11}$$

On one hand, the transmitter is modeled by a prescribed displacement boundary condition at $x_3 = 0$, whose distribution is uniform and applied normal to the transducer contact area. The temporal shape of the excitation is a sinusoidal oscillation at 5 MHz modulated by a uniform window. On the other hand, the receiver is modeled as a semi-infinite layer, in order to avoid any reflections that could perturb the detection of the transmitted wave. The corresponding boundary condition for a semi-infinite elastic medium is expressed by the radiation energy condition. By making use of the Fourier transform, the excitation is expressed as a wave displacement in the frequency-domain, and each harmonic component is treated separately. Given equation system (10) for each harmonic component n and inserting the boundary conditions allow to compute the solution $\tilde{u}_N^{(n)}(h,\omega)$ in the frequency-domain. Finally, the wave displacement at the receiver position $u(h,t)$ is calculated in the time-domain using the inverse Fourier transform.

2.5. Inverse problem

A model-based inverse problem (IP) is applied to reconstruct the values of the parameters ($\mathbf{p}$) that best fit the experimental measurements. A good review is provided by Tarantola [34] for the theory of inverse problems, particularly concentrating on Monte Carlo and least-squares methods. Another review of more specific issues within the elasticity is given by Bonnet and Constantinescu [4].

2.5.1. General scheme

The characterization of inverse problem or search of the mechanical parameters is carried out with an iterative strategy based on the minimization of the discrepancy between the measured and numerically predicted waveforms, labeled as $\Phi^x(t)$ and $\Phi(t)$, respectively. The discrepancy is a vector of values or a function that can be discretized. Since two vectors cannot be compared directly, a scalar number (called cost functional) is derived from them, in order to be able to minimize that discrepancy according to the scheme in Fig. 6.

A *residual* $r(t)$ that represents the mismatch or *discrepancy* $\Phi^x(t) - \Phi(t)$ between the experimental and synthesized measurements is defined as,

$$r(t) = (\Phi^x(t) - \Phi(t)) \tag{12}$$

2.5.2. Parametrization

Since the goal of the inverse problem is to find the damage state of the system, it should be parametrized. Parametrizing can be interpreted as representing the model $m = m(\mathbf{p})$ by a finite set of parameters $\mathbf{p} = \{p_m\}$. While doing the parametrization, a *priori* information is included in the model space, which effectively reduces its dimension to that of $\mathbf{p}$. It can be defined within the con-

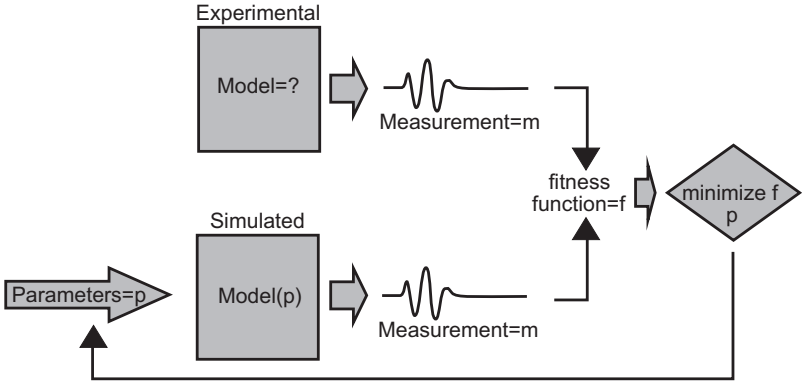

Fig. 6. Scheme of the setup for the numerical model.

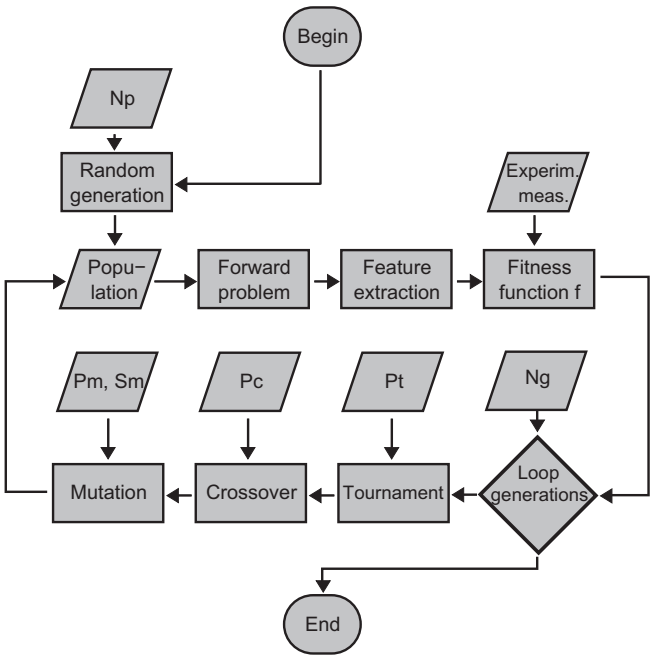

Fig. 7. Flow chart of the inverse problem solution by genetic algorithms. N_p: number of individuals in population; N_g: number of generations; P_t: probability of tournament; P_c: probability of crossover; P_m: probability of mutation; it S_m: scale of mutation.

text of inverse problems as a description or characterization of the sought information with a reduced set of variables. The damage in each layer/interface m is assumed to be correlated with Young modulus $E_m \to \overline{E}_m$ and Rayleigh damping $\alpha_m \to \overline{\alpha}_m$ reductions, respectively. The parameter $\mathbf{p} = \{p_m\}$ that characterizes the damage is defined in a non-dimensional and logarithmic scale, in order to improve the conditioning of the algorithm,

$$\overline{E}_m = E_m e^{p_m}, \quad \overline{\alpha}_m = \alpha_m e^{p_m} \tag{13}$$

where p_m ranges from $[0, -3]$, and thus corresponds to a decrease of the properties from 0 to approximately 95%.

2.5.3. Cost functional

There are many options to design a cost functional. The necessary conditions are (a) that a full coincidence of prediction and measurement (zero discrepancy) should coincide with the absolute minimum of the cost functional; and (b) that of uniqueness of this minimum. This quadratic or least squares type definition is meaningful in a probabilistic sense, as well as in an algebraic sense as a measure of a distance between bad and good results. The *cost functional* f or fitness function is chosen after a residual vector $r(t)$ as,

$$f = \frac{1}{2}\int_0^T |r(t)|^2 dt \tag{14}$$

where T is the time period of the captured signals. In contrast to gradient-based algorithms, for which the CF is defined as f, when the minimization is carried out by genetic algorithms, the CF is usually defined in an alternative way as f^L:

$$f^L = \log(f + \epsilon) \tag{15}$$

where ϵ is a small non-dimensional value (here adopted as $\epsilon = 10^{-16}$) that ensures the existence of f^L when f tends to zero. In addition, as it was argued by Gallego and Rus [9] and Gallego et al. [8], this

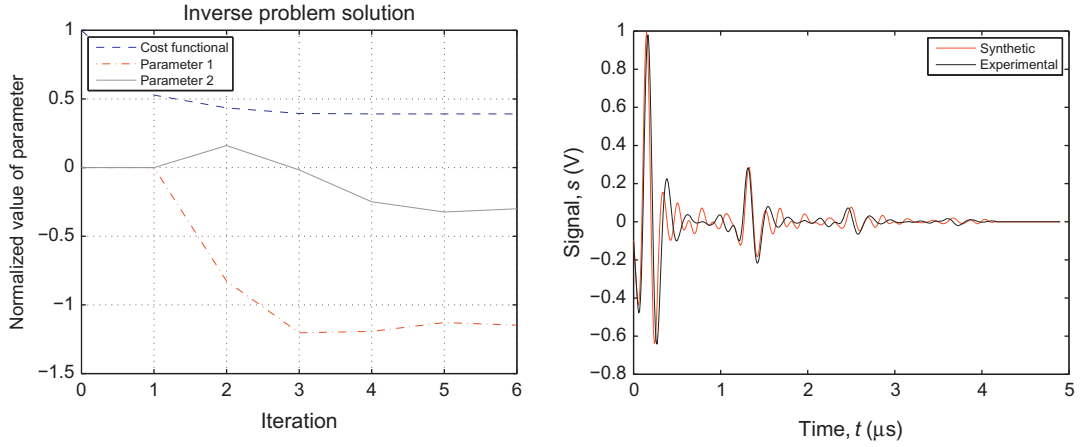

Fig. 8. Left plot shows the initial guess by the BFGS. Right plot shows the final calibration of the simulated model.

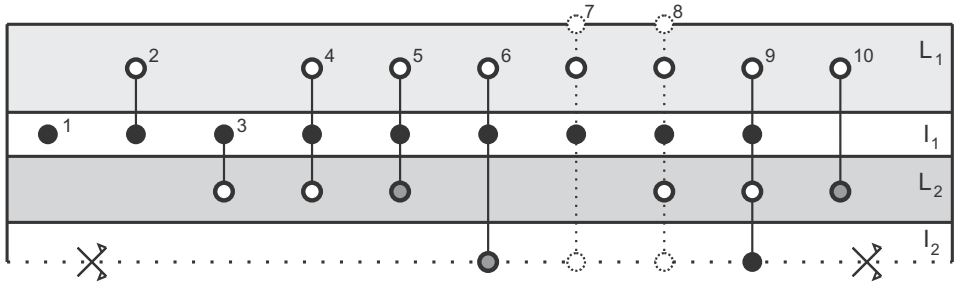

Fig. 9. Parameters configuration over the symmetric specimen: representation of 10 cases used to predict the damage. The black circles denote parameter 1, while the white and the gray ones denote parameters 2 and 3, respectively. The discontinuous line of cases 7 and 8 denotes a damping parameter assignation over the structure.

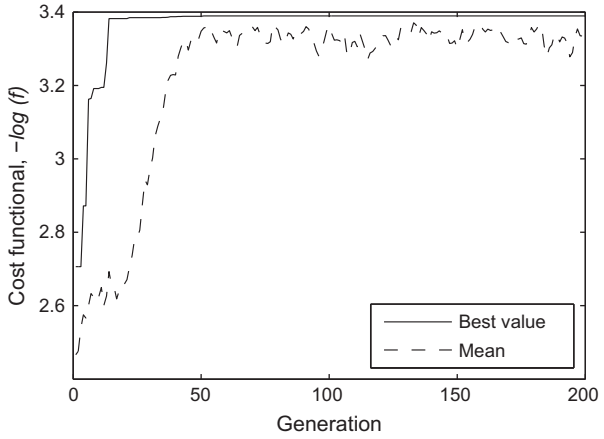

Fig. 10. Evolution of the GA in the case of 50 individuals and 200 generations.

Table 5
Parameters used for the GA search algorithm.

Parameter	Value
Population size	50
Number of generations	200
Probability of crossover	0.80
Probability of mutation	0.10
Probability of selection	0.70

definition of the CF increases the convergence speed of the selected minimization algorithm.

2.5.4. Search algorithms

Finally, the parameters that characterize the damage are found by a search algorithm that minimizes the CF (which is given in terms of the parameters (**p**) that best fit the characterization of the defect with the criteria of measurement similarity). The search is formulated following [17] and the maximum likelihood solution of the inverse problem of defect evaluation can be stated as a minimization problem, that can be constrained to find (**p**) such that:

$$\hat{p} = \min_{p} f^{L}(p) \tag{16}$$

Broyden–Fletcher–Goldfarb–Shanno (BFGS) gradient-based algorithm is used in the calibration of the model while genetic algorithm [10] techniques are employed to minimize Eq. (16) and to obtain the IP output (see Fig. 7), since in [29] it was concluded that GA guarantees convergence, whereas gradient-based algorithms strongly depend on the initial guess that needs to be provided. The GA is a heuristic optimization technique based on the rules of natural selection and genetics. It simulates the mechanism of survival competitions: the superiors survive while the inferiors are eliminated. First, a population of individuals (called chromosomes) is randomly generated. The population comprises a group of chromosomes that represent possible solutions in a problem domain. Each solution is evaluated by computing its cost functional, for which one forward problem is solved independently. Genetic operators such as crossover and mutation are applied to obtain a child

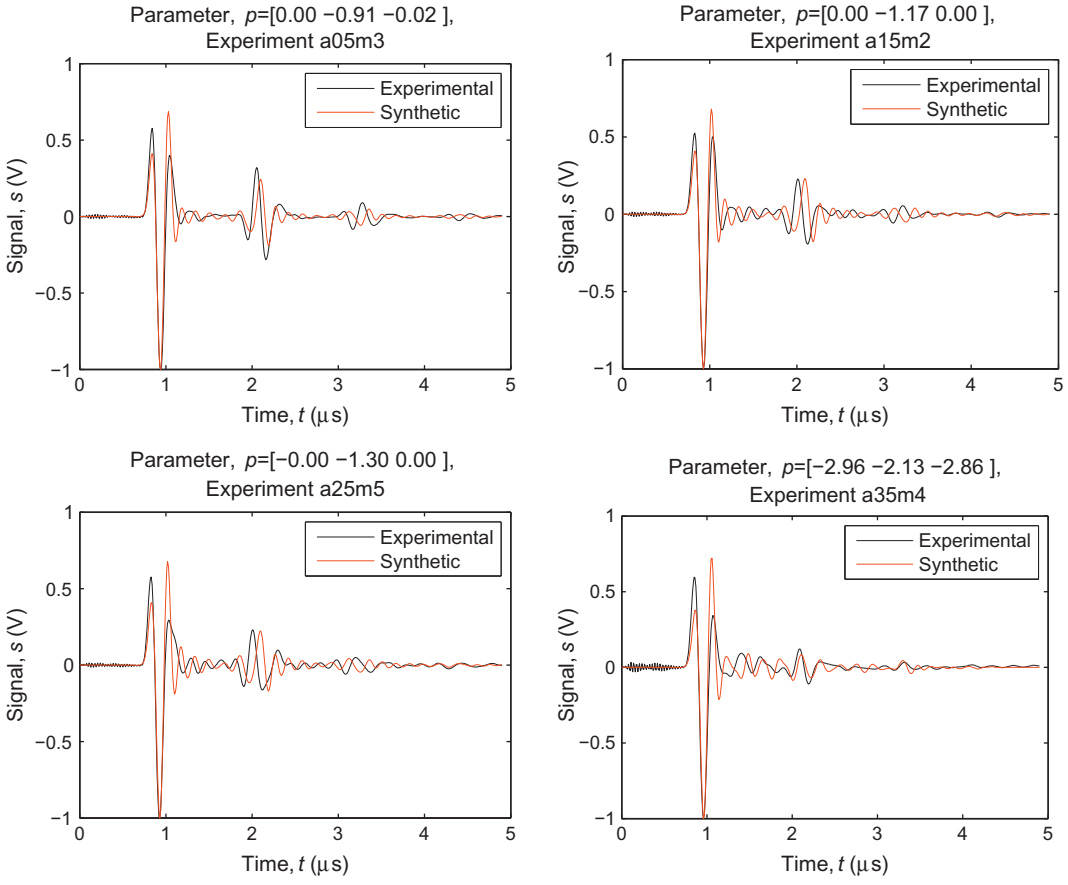

Fig. 11. Inverse problem solution (with 3 parameters) for specimen-A with four levels of damage, which shows comparison between experimental and simulated measurements.

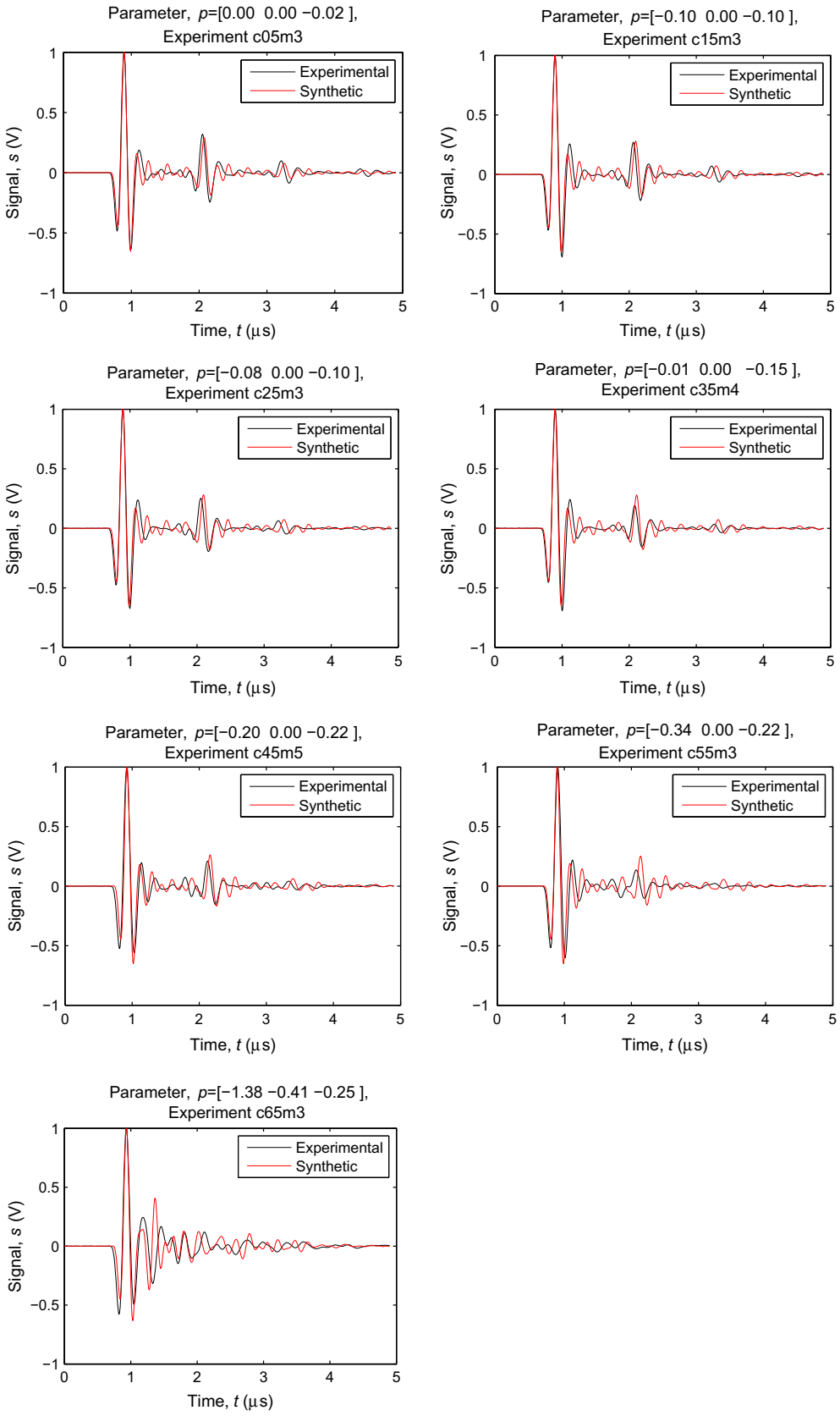

Fig. 12. Inverse problem solution (with 3 parameters) for specimen-C with seven levels of damage, which shows comparison between experimental and simulated measurements.

population. Then, the child chromosomes with higher fitness replace some of their parent chromosomes. The process runs until a stopping criterion (for instance a number of generations) is reached.

The description and implementation of the used algorithm is detailed in previous papers from the authors [23], where it has been used in the same form but for other definitions of the discrepancy or cost function or for different models and applications.

3. Results

3.1. Model calibration

The first problem tackled is the calibration of the numerical model that solves the forward problem. This is done by a matching procedure, in which two parameters (Young modulus and damping ratio of the polymer matrix, assuming the fiber fraction and

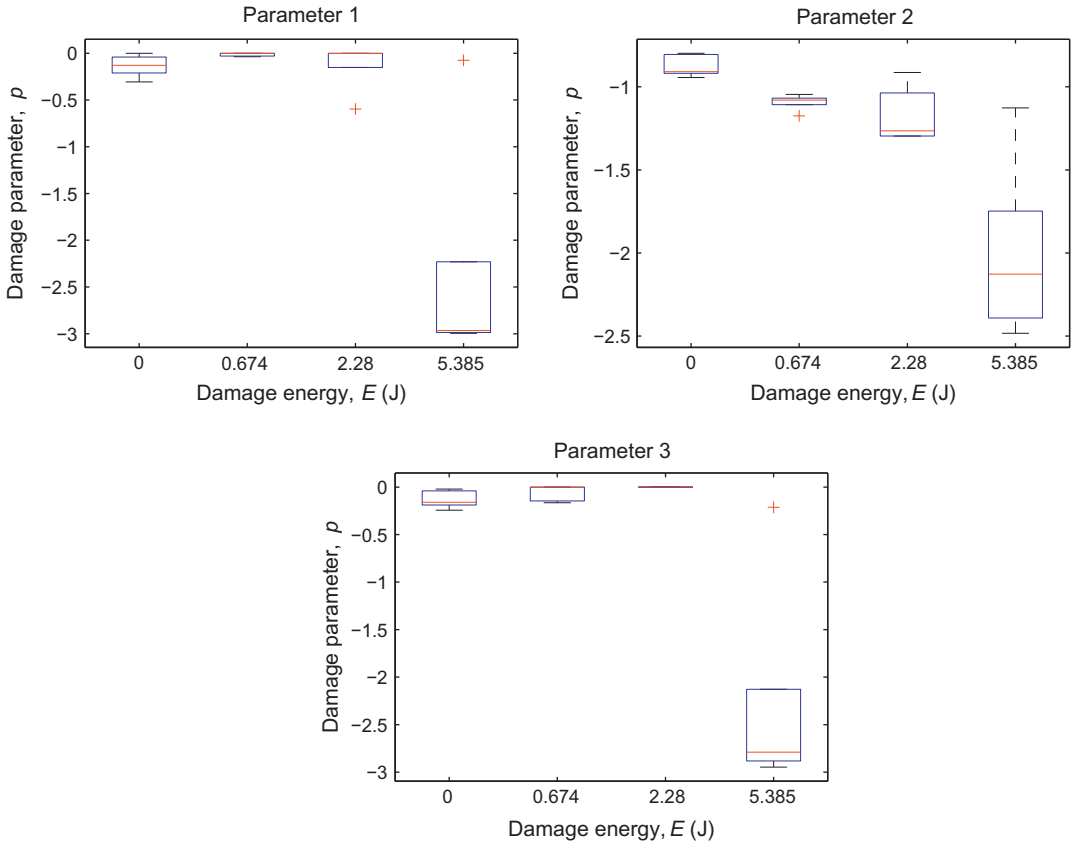

Fig. 13. Specimen 'A', parameter 1: shows that low energy not affects seriously the first four layers and the damage starts only after growing impact (∼5 [J]), parameter 2: shows that there is a clear delamination growth in the second interface increasing with the increase of the impact energy, parameter 3: shows that low energy not affects seriously at the last layer and the damage starts only after growing impact (∼5 [J]).

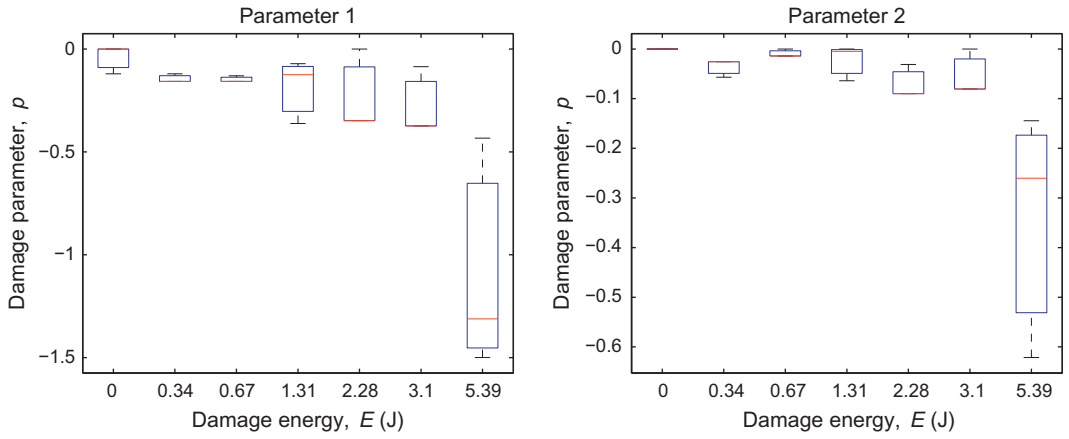

Fig. 14. Specimen 'C', parameter 1: shows that delamination occurs in the first and the last interfaces and it is increasing with the damage level, parameter 2: shows that low energy not affects seriously at the layers and the damage starts only after growing impact (∼5 [J]).

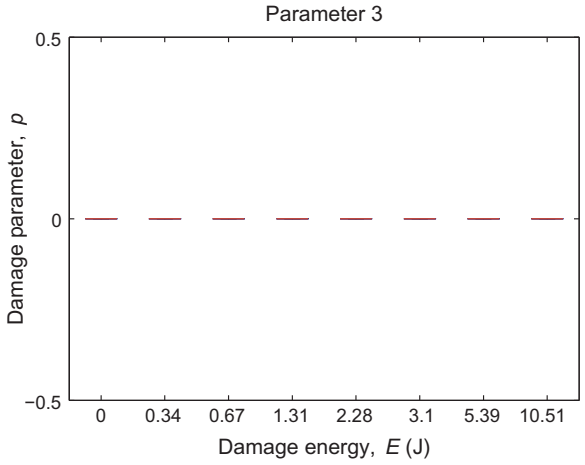

Fig. 15. Damage correlation parameter of Rayleigh damping.

densities characterized above) of the simulated model are adjusted by a BFGS search algorithm to find the non-damaged values for both parameters, as highlighted in Fig. 8.

Comparison of Signals: Experimental and synthetic signals have been compared up to the time for which there are no reflections from the boundaries of specimens, and a fairly good matching was obtained. The time at which the waveform starts denotes the time of arrival (time taken by the wave to reach the receiver). After the time of arrival of the wave front, the obtained signal is a superimposition of transmitted and reflected waves from the interfaces.

3.2. Identification of damage distribution

A number of hypothesis on the selection and distribution of damage along layers and interfaces were made as summarized in Fig. 9 for specimen C. The parametrized inverse problem was solved for each hypothesis and damage level. The determination of the correct distribution of damaged layers/interfaces was selected by falsifying the hypothesis yielding contradictory results in the sense that either the synthetic to experimental signal matching was not achieved, or the damage parameters evolution was not monotonically dependent on damage level. For the case of specimen C, since the composite specimens used in this study are symmetric in their layers, thickness, fiber direction and their mechanical properties, the parameters used to detect the damage were assumed to behave symmetrically, since it is not possible to distinguish asymmetry using a linear model.

The conclusion of the comparison was, that for specimen A, layers 1 (counting from the impacted side) and 4 degrade following a common parameter, a delamination between 4 and 5 appears following a second independent parameter, and layer 5 degrades following a third independent parameter. For specimen C, layers 1 and 4 degrade following one parameter, and interfaces 1–2 and 3–4 delaminate following a second independent parameter. These results are in agreement with the expectation that delamination concentrates mostly in the last interface opposite to the impacted side. Their evolution with increasing impact energy is studied in next section.

3.3. Inverse problem

To verify the convergence of GA, Fig. 10 shows the evolution along each generation of the best individual of the population, and their average.

A number of parameters have to be adjusted in the GA algorithm to optimize its computational efficiency and guarantee good convergence to a global optimum, while establishing a compromise between inverse problem error and computational cost. Table 5 summarizes the selected GA configuration parameters according to the results obtained above.

Figs. 11 and 12 show the final values of damage parameters computed by the genetic algorithms and the matching of the damaged experimental signal with the synthetic one.

3.4. Sensitivity study

3.4.1. Sensitivity to damaged interface/layer

The parameters of the model are adjusted as explained above to detect the location of the damage in layers or interfaces, where the level of damage p is plotted against the values of the input parameter (Young modulus E). This is done by adding a gaussian noise with zero mean and standard deviation as a percentage of the RMS of the measurement signal. It shows that the technique is highly robust against a high noise level as illustrated in Figs. 13 and 14 where damage correlation parameters 1–3 highlight the following result: The elastic modulus consistently decreases while increasing the damage level.

A careful interpretation of the figures allow to observe that the delamination in the interfaces of the laminated composites occurs at the early stages of the impact energies and increase with the damage level. In contrast, it is more complicated to prove

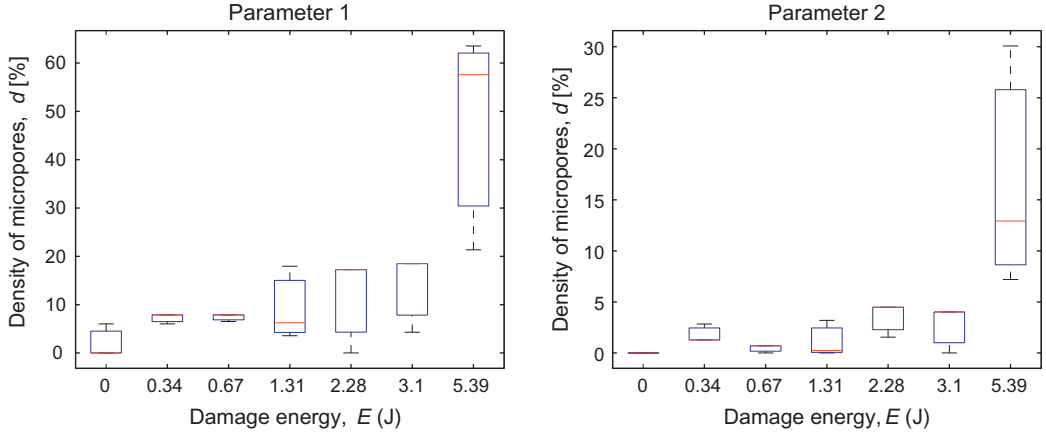

Fig. 16. Damage correlation parameters of degradation evolution within micropores density increase.

significant damage at a low energy impact in the layers of the material even if there is a small reduction in the parameter presenting the damage in such layers. This reduction can be explained as an error due to the measurements noise, uncertainty in the numerical model or the calculated mechanical properties.

3.4.2. Sensitivity to Rayleigh damping

The two models used for both specimens A and C proved that the Rayleigh damping is not correlated to impact damage level as illustrated in Fig. 15.

3.4.3. Micromechanical interpretation

The complex nature of the composite material systems almost surely dictates that a micromechanical analysis is needed to relate the physical properties and response at the global level to the properties and response of the constituent materials (including the interface).

The Mori–Tanaka method has received attention recently in the micromechanics community. It is based on the original work of Mori and Tanaka [19] and has been used by Taya and Mura [37] and Taya and Chou [36] among others in predicting the effective thermal, electrical, or mechanical properties of composites. A closed-form solution was derived for the stress and energy distribution in and around spheroidal inclusions and voids at finite concentrations by combining Eshelby's solution for an ellipsoidal inclusion and the Mori–Tanaka concept of average stress in the matrix.

The non-dilute stresses in the fibers and matrix, derived by using the Mori–Tanaka method, which is presented in [41], shear modulus G and Bulk modulus K can be expressed as a function of damage variable, the value of this damage parameter D is extracted to plot the evolution of degradation in multilayered composites by micropores density with the increase of the impact damage realized as illustrated in Fig. 16.

$$D = \frac{2\left(1-\frac{\bar{E}}{E}\right)(5\nu-7)}{2(5\nu-7)+\frac{\bar{E}}{E}(15\nu^2+2\nu-13)} \tag{17}$$

A consistent correlation is shown between a moderate density of micropores inside the degraded layers, a large density of micropores in delaminated interfaces, and the impact energy.

4. Conclusions and future work

This work shows that the ultrasonic wave propagation phenomena can be exploited to reconstruct the mechanical properties of the composite materials they travel through. This requires a robust inverse problem solution technique as well as a reliable forward model of the propagation. A numerical method to determine the location and extent of defects in layered composite material is developed by combining the solution of an identification inverse problem, using genetic algorithms to minimize a cost functional. A method to determine the identifiability of each parameter is assessed and the preliminary results exhibit the feasibility of the method. To asses the potential of the proposed reconstruction technique, the different sources of errors have been isolated (experimental, modelling and inversion algorithm). A sensitivity analysis has shown that some parameters, like Rayleigh damping are not dependent on damage, while the Young modulus can be reasonably well identified. This technique is proved experimentally consistent, despite limitations in that results are sensitive to uncertainties of interfacial couplant and contact conditions. The results show that the distribution of damage and its structural severity can be anticipated at a significantly earlier stage than commercial techniques. Verification of feasibility of the method to determine interface debonding by including an interface damage factor model. The technique allows to determine to an order of magnitude of 0.6 J the energy needed to start each damage. The sensitivity of the technique allows to determine with 15% uncertainty the identifiable damage in terms of microvoids volume fraction at interfaces, and with 3% uncertainty the microvoid fraction responsible for layer degradation. Ongoing works may include the study of the influence of the hygrothermal effects on the composite material degradation.

References

[1] Allen D, Harris C, Groves S. A thermomechanical constitutive theory for elastic composites with distributed damage – I. theoretical development. Int J Solids Struct 1987;23:1301–18.

[2] Allen D, Lee J-W. Matrix cracking in laminated composites under monotonic and cyclic loadings. Compos Eng 1991;1:319–34.

[3] Bochud N, Gómez Ángel M, Rus G, Carmona JL, Peinado AM. Robust parametrization for non-destructive evaluation of composites using ultrasonic signals. In: Proc of IEEE international conference on acoustics, speech, and signal processing, Prague; 2011. p. 1789–92.

[4] Bonnet M, Constantinescu A. Inverse problems in elasticity. Inverse Probl 2005;21(2):R1–R50.

[5] Chang J, Zheng C, Ni QQ. The ultrasonic wave propagation in composite material and its characteristic evaluation. Compos Struct 2006;75:451–6.

[6] Cretu N, Nita G. Pulse propagation in finite elastic inhomogeneous media. Comput Mater Sci 2004;31:329–36.

[7] Fuentes B, Carmona JL, Bochud N, Gomez AM, Peinado AM. Model-based cepstral analysis for ultrasonic non-destructive evaluation of composites. In: Proc of IEEE international conference on acoustics, speech, and signal processing, Kyoto; 2012. p. 1–4.

[8] Gallego R, Comino L, Cabello AR. Material constant sensitivity boundary integral equation for anisotropic materials. Int J Numer Methods Eng 2006;66(12):1913–33.

[9] Gallego R, Rus G. Identification of cracks and cavities using the topological sensitivity boundary integral equation. Comput Mech 2004:33.

[10] Goldberg D. Genetic algorithms in search, optimization and machine learning. Reading, Massachussets, etc: Addison-Wesley Publ.; 1989.

[11] Hashin Z. Analysis of cracked laminates: a variational approach. Mech Mater 1985;4:121–36.

[12] Kinra VK, Iyer VR. Ultrasonic measurement of the thickness, phase velocity, density or attenuation of a thin viscoelastic plate – Part I: the forward problem. Ultrasonics 1995;33(2):95–109.

[13] Kyriazoglou C, Guild F. Quantifying the effect of homogeneous and localized damage mechanisms on the damping properties of damaged GFRP and CFRP continuous and woven composite laminates-an FEA approach. Composites: Part A 2008;36:367–79.

[14] Lee SY, Rus G, Park T. Detection of stiffness degradation in laminated composite plates by filtered noisy impact testing. Comput Mech. 2007:1–15.

[15] Lee SY, Rus G, Park TH. Quantitative nondestructive evaluation of thin plate structures using the complete frequency from impact testing. Struct Eng Mech 2008;28:525–48.

[16] Lee SY, Wooh SC. Detection of stiffness reductions in laminated composite plates from their dynamic response using the microgenetic algorithm. Comput Mech 2005;36:320–30.

[17] Lee SY, Wooh SC. Waveform-based identification of structural damage using the combined FEM and microgenetic algorithms. J Struct Eng ASCE 2005;131(9):1464–72.

[18] Mal A, Yin C-C, Bar-Cohen Y. Ultrasonic nondestructive evaluation of cracked composite laminates. Compos Eng 1991;1:85–101.

[19] Mori T, Tanaka K. Average stress in matrix and average elastic energy of materials with misfitting inclusions. Acta Metall 1973;21:571–4.

[20] Nag A, RoyMahapatra D, Gopalakrishnan S. Identification of delamination in composite beams using spectral estimation and a genetic algorithm. Smart Mater Struct 2002;11:899–908.

[21] Nairn JA, Hu S. The initiation and growth of delaminations induced by matrix microcracks in laminated composites. Int J Fract 1992;57:1–24.

[22] Olsson R, Donadon MV, Falzon BG. Delamination threshold load for dynamic impact on plates. IJSS 2006;43:3124–41.

[23] Palma R, Rus G, Gallego R. Probabilistic inverse problem and system uncertainties for damage detection in piezoelectrics. Mech Mater 2009;41:1000–16.

[24] Rattanachan S, Miyashita Y, Mutoh Y. Fabrication of piezoelectric laminate for smart material and crack sensing capability. Sci Technol Adv Mater 2005;6(6):704–11.

[25] Reddy J, Miravete A. Practical analysis of composite laminates. 1st ed. New York: CRC Press, Inc.; 1995.

[26] Ruosi A. A nondestructive detection of damage in carbon fibre composites by SQUID magnetometry. Phys Status Solidi 2005;2:1533–55.

[27] Rus G, Lee S, Gallego R. Defect identification in laminated composite structures by BEM from incomplete static data. Int J Solids Struct 2005;42:1743–58.
[28] Rus G, Lee SY, Chang SY, Wooh SC. Optimized damage detection of steel plates from noisy impact test. Int J Numer Methods Eng 2006;68:707–27.
[29] Rus G, Palma R, Perez-Aparicio JL. Optimal measurement setup for damage detection in piezoelectric plates. Int J Eng Sci 2009;47:554–72.
[30] Shen Q, Omar M, Dongri S. Ultrasonic NDE techniques for impact damage inspection on CFRP laminates. J Mater Sci Res 2011;1(1):2.
[31] Staszewski W. Intelligent signal processing for damage detection in composite materials. Compos Sci Technol 2002;62(7–8):941–50.
[32] Talreja R. A continuum mechanics characterization of damage in composite materials. Proc R Soc Lond A 1985;399:195–216.
[33] Talreja R. Stiffness properties of composite laminates with matrix cracking and interior delamination. Eng Fract Mech 1986;25:751–62.
[34] Tarantola A. Inverse problem theory. SIAM; 2005.
[35] Tarantola A, Valette B. Inverse problems = quest for information. J Geophys 1982;50:159–70.
[36] Taya M, Chou T. On two kinds of ellipsoidal inhomogeneities in an infinite elastic body: an application to a hybrid composite on two kinds of ellipsoidal inhomogeneities in an infinite elastic body: an application to a hybrid composite. Int J Eng Sci 1981;17:553–63.
[37] Taya M, Mura T. On the stiffness and strength of an aligned short-fiber reinforced composite containing fiber-end cracks under uniaxial applied stress. ASME J Appl Mech 1984;48:361–7.
[38] Williams KV, Vaziri R, Poursartip A. A physically based continuum damage mechanics model for thin laminated composite structures. Int J Solids Struct 2003;40:2267–300.
[39] Xu Y, Liu G. Detection of flaws in composites from scattered elastic-wave field using an improved μGA and a local optimizer. Comput Methods Appl Mech Eng 2002;191:3929–46.
[40] Yang Z, Liu G, Lam K. An inverse procedure for crack detection using integral strain measured by optical fibers. Smart Mater Struct 2002;11:72–8.
[41] Yeh H-Y, Cheng J-H. NDE of metal damage: ultrasonics with a damage mechanics model. Int J Solids Struct 2003;40:7285–98.
[42] Zhang R, Wan M, Cao W. Parameter measurement of thin elastic layers using low-frequency multi-mode ultrasonic lamb waves. IEEE Trans Instrum Meas 2001;50(5):1397–403.